A Multiplexed Impedance Analyzer for Characterizing Polymer-Coated QCM Sensor Arrays

Christopher A. Mills, Kevin T. C. Chai, Mark J. Milgrew, *Member, IEEE*, Andrew Glidle, Jonathan M. Cooper, and David R. S. Cumming, *Member, IEEE*

***Abstract*—This paper describes the development and evaluation of a custom-built impedance analyzer, which uses a multiplexing bridge circuit to characterize an array of polymer-coated quartz crystal microbalance (QCM) sensors. The analyzer is constructed on a single printed circuit board with minimum components and is sufficiently compact for integration into a handheld format. The custom-built device is used to observe the changes that occur in QCM sensors when experimental conditions such as polymer coating film thickness, odorant vapor pressure, and relative molecular mass are varied. An equivalent electric circuit for a QCM is used to model the conductance and susceptance data captured by the analyzer. The measured response of an array of QCM sensors demonstrates that the custom-built device is a suitable instrument for detecting different gases and understanding polymer–vapor interactions.**

***Index Terms*—Array, gas detector, impedance analyzer, polymer coated, quartz crystal microbalance (QCM), sensor.**

I. Introduction

SHEAR acoustic wave devices such as quartz crystal microbalance (QCM) sensors have been used in a range of electronic nose [1], [2] and electronic tongue [3] sensor systems. A QCM sensor consists of a quartz crystal, which is coated with an analyte-sensitive polymer. The analyte is absorbed into the surface of the polymer coating, increasing the mass of the QCM sensor, and hence, resulting in a change in resonant frequency [4]. Thus, for a thin rigid film, the most common method of data acquisition from the QCM sensor is to measure the resonant frequency [5]. For QCMs with viscoelastic films, it is necessary to treat the device as a hybrid sensor and combine the simultaneous measurement of resonant frequency shift with the resistance change of the polymer coating [6].

A simple QCM sensor relies solely on the measurement of the self-resonant frequency, typically using an oscillator circuit for which the QCM is the tuning device [7]. However, it is well known that the impedance spectrum of a QCM sensor contains a wealth of detailed information that is particularly valuable in sensor applications [8]. Impedance analysis in combination with modern electronics and data extraction software can provide a sensor system solution. In particular, the measurement of the change in the resonant frequency of the quartz crystal and the damping of its vibration can be extracted from the electrical impedance spectrum.

Currently, impedance analysis can be performed with a bench instrument (for example, an inductance–capacitance–resistance (LCR) meter) [9]. There have also been several circuits and methods developed for determining the impedance parameters of loaded quartz crystal resonators [10], [11]. For many applications though, it is desirable not only to extract the impedance spectrum for a single QCM sensor but also to make the same measurement on an array of sensors that have been treated to give diverse functional behaviors [12]. Furthermore, it is beneficial to miniaturize the instrumentation to the point where it may conveniently be built into a handheld format.

In this paper, we present the development and evaluation of a prototype custom-built impedance analyzer for characterizing arrays of polymer-coated QCM sensors. A multiplexing bridge circuit is used to allow the analyzer to measure the complex impedance of each sensor in the array. The complete system consists of a small number of discrete components, which can easily be adapted into a portable handheld format. The performance of the analyzer is evaluated by observing the interactions between different polymer-coated QCM sensors and vapors. These measurements are then compared and contrasted with the underlying physics and chemistry of the QCM sensors.

II. System Design

A. Custom-Built Impedance Analyzer

The impedance analyzer is a bridge circuit designed specifically to measure the impedance of a QCM [Fig. 1(a)]. The circuit is based around a standard four-terminal or Kelvin bridge configuration, which is used to reduce the effect of stray or parasitic impedances. Overall, the system comprises of an ac source and voltage-measuring circuit for the QCM, signal buffering, in-phase quadrature (IQ) demodulators for the current and voltage signals, a data converter, and an interface to a PC. All of the electronic components are carefully selected so that they have sufficient slew rate and bandwidth to minimize distortion.

The circuit uses a sweepable 5-MHz direct digital frequency synthesizer (DDFS) that drives a current into the QCM via a source resistor R_S. The QCM is placed in feedback around an amplifier, the output of which follows the voltage drop across the crystal. The voltage signal is buffered, whereas the current is detected by a differential buffer amplifier connected across R_S. The voltage and current signals are demodulated for in-phase

Manuscript received March 8, 2005; accepted January 24, 2006. This work was funded by the Engineering and Physical Sciences Research Council, U.K. The associate editor coordinating the review of this paper and approving it for publication was Prof. Ralph Etienne-Cumming.

C. A. Mills is with the Nanobioengineering Laboratory, Barcelona Science Park, 08028 Barcelona, Spain (e-mail: cmills@pcb.ub.es).

K. T. C. Chai, M. J. Milgrew, A. Glidle, J. M. Cooper, and D. R. S. Cumming are with the Department of Electronics and Electrical Engineering, University of Glasgow, G12 8LT Glasgow, U.K. (e-mail: kevintc@elec.gla.ac.uk; mark@elec.gla.ac.uk; a.glidle@elec.gla.ac.uk; j.cooper@elec.gla.ac.uk; d.cumming@elec.gla.ac.uk).

Digital Object Identifier 10.1109/JSEN.2006.877936

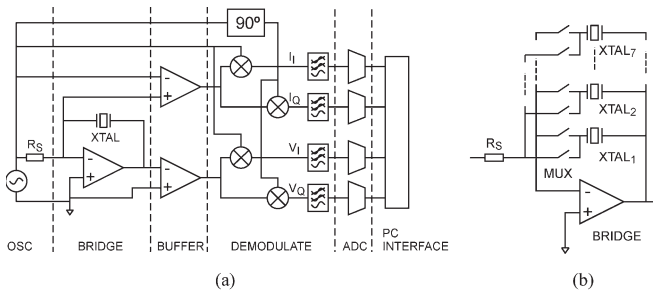

Fig. 1. Block diagram of the custom-built impedance analyzer. (a) System. (b) Multiplexing configurations.

and quadrature terms. These terms are then low-pass-filtered, converted to ten-bit digital values, and input to the PC interface. Additional circuitry includes an array of video multiplexers [Fig. 1(b)], which enables switching between different QCMs and the bridge. The multiplexers are inserted into the bridge circuit so that their on-resistance is not incorporated unintentionally into the impedance readings of the sensors.

With the exception of the DDFS (which could be implemented on a single chip), the impedance analyzer is built on a single printed circuit board (PCB). Therefore, the system offers the additional feature that it can potentially be integrated into a portable handheld device. For the purpose of experiments, a signal generator under the control of a PC is used to drive the circuit. The PC uses a general purpose interface bus (GPIB) and customized control software written in C to capture data from the impedance analyzer circuit. The software also controls the video multiplexers and performs standard impedance transformations to yield signal spectra.

The impedance analyzer is a conventional homodyne device and produces four signals that describe the real and imaginary parts of the QCM current and voltage. These data are algebraically manipulated to give the potential drop $(|V|\angle\theta)$ across the crystal and the current $(|I|\angle\phi)$ through the crystal. The impedance and its associated phase $(|Z|\angle\varphi)$ are calculated using

$$|Z|\angle\varphi = \frac{|V|}{|I|}\angle(\theta - \phi). \tag{1}$$

The magnitude of the impedance is calculated using the design values of the circuit components, and the phase of the impedance is calculated as an absolute value. The instrument gives a magnitude resolution of less than 0.5% and a phase resolution of 25 mrad. The dynamic range in each case is limited by an eight-bit analog-to-digital converter (ADC), which yields a zero to full-scale range of 5 kΩ for the magnitude of the impedance and 2π rad for the phase of the impedance. The resolution of the frequency measurement is better than 1 Hz.

B. QCM Sensors

The QCMs (5 MHz fundamental, HC49-4H series AT-cut crystals, Euroquartz Ltd., U.K.) are supplied in a hermetically sealed can, which is removed by filing down to reveal the bare rectangular QCM (width 2 mm, length 8 mm, thickness 150 μm, and oscillating area 10 mm^2). A polymer coating is spin-cast onto each QCM from a solution of the polymer (between 1% and 5% v/v) in toluene, dichloromethane (DCM), or tetrahydrofuran (THF) ($\geq$ 99.8% purity, Sigma-Aldrich Ltd., U.K.). The polymer solution is applied to the QCMs using a dropping pipette and spun at 7000 rpm for 30 s to form a layer thickness between 200 and 700 nm, depending on the polymer type. The crystals are left to stand at room temperature (23 °C) and in normal humidity conditions (ca. 65%) for 24 h to allow the solvent to evaporate from the polymer. The baking step is omitted to avoid damaging the electrodes and the connections attached to the crystals.

TABLE I
POLYMER ABBREVIATIONS AND SOLVENTS

Polymer	Abbreviation	Solvent
Poly(styrene)	PS	Toluene
Poly(ethylene-*co*-methyl acrylate) *(29% methyl acrylate)*	PE-*co*-MA	Toluene
Poly(vinyl chloride)	PVC	THF
Poly(vinyl phenyl ketone)	PVPK	Toluene
Poly(ethylene-*co*-vinyl acetate) *(33% vinyl acetate)*	PE-*co*-VA	Toluene
Poly(methyl methacrylate)	PMMA	Toluene
Poly(vinyl pyrrolidone)	PVP	DCM

The polymers used to fabricate the sensors are given in Table I, along with the corresponding solvent used to dissolve the polymer. The polymers include ketone, ester, and chlorinated systems and are all used as supplied (Sigma-Aldrich). The headspace of the sample alcohols (Sigma-Aldrich) is investigated using modified sampling bottles (1 L, 500 mL, and 250 mL). The sensors are held in the screw cap, and an interface to the impedance analyzer electronics is achieved via a connection through the cap. The experiments are carried out at room temperature and in normal humidity conditions. The sensors are restored to baseline conditions at the start of each set of experiments by exposure to a continuous stream of nitrogen for 30 min. When exposed to an analyte, the sensors take approximately 3 min to reach their equilibrium.

III. EXPERIMENTAL RESULTS

A typical plot of the conductance G and the susceptance B of an uncoated 5-MHz QCM is produced using the custom-built impedance analyzer [Fig. 2(a)] and an HP 4192A LF impedance analyzer [Fig. 2(b)] for comparison. In each case, the data are recorded at 2-Hz intervals between 4.9992 and 5.0002 MHz. The plots reveal a maximum conductance of 21.57 mS at 4 999 526 Hz and 28.05 mS at 4 999 624 Hz for the custom-built analyzer and the HP analyzer, respectively. Logarithmic data sampling is used to expand the measurement range over at least four decades in frequency. This reveals that the susceptance has an underlying element that increases as the measurement frequency increases (Fig. 2, inset graphs). For the remainder of the experimental work, the data are captured using the custom-built impedance analyzer.

QCMs are coated with polymer films spun from increasingly concentrated solutions of polyethylene-co-vinylacetate (PE-co-VA) to illustrate the effect of increasing the mass of polymer

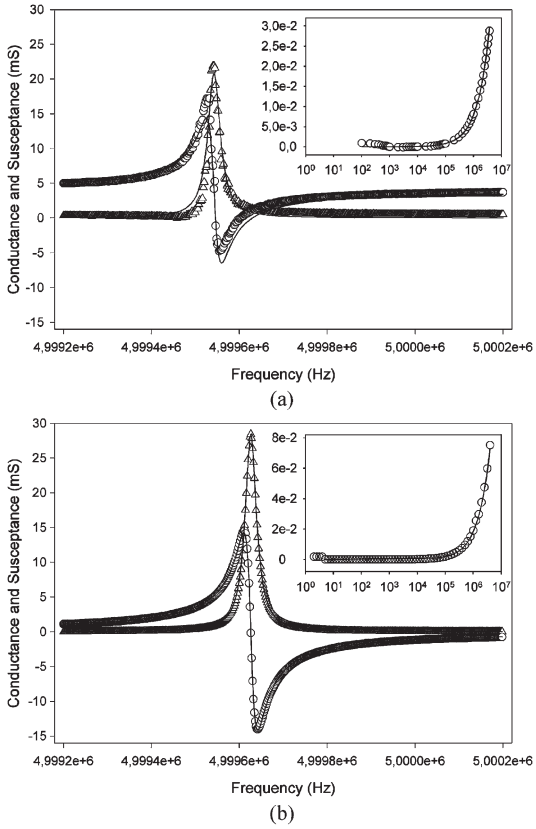

Fig. 2. Graph of conductance (Δ) and susceptance ($\circ$) versus frequency for an uncoated QCM. The solid lines represent the mathematical fitting of the experimental data using (2) and (3). The inset graphs illustrate the relationship between background susceptance and frequency. (a) Custom-built impedance analyzer. (b) HP 4192A LF impedance analyzer.

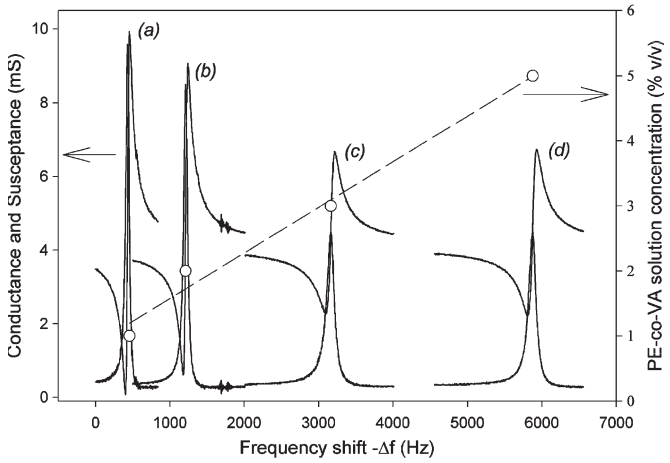

Fig. 3. Graph of conductance and susceptance versus frequency shift (solid lines) for QCMs loaded with PE-co-VA, spin-cast from (a) 1%, (b) 2%, (c) 3%, and (d) 5% v/v polymer solutions. The dashed line is a plot of PE-co-VA solution concentration versus frequency shift ($\circ$).

on the QCM (Fig. 3). The resultant frequency shift $-\Delta f$ is the difference in resonance between the uncoated and coated QCM. As the mass of the polymer deposited on the QCM increases (from 1% v/v to 5% v/v PE-co-VA solutions in toluene), the resonant frequency moves to lower frequencies in an approximately linear fashion. At the same time, the frequency

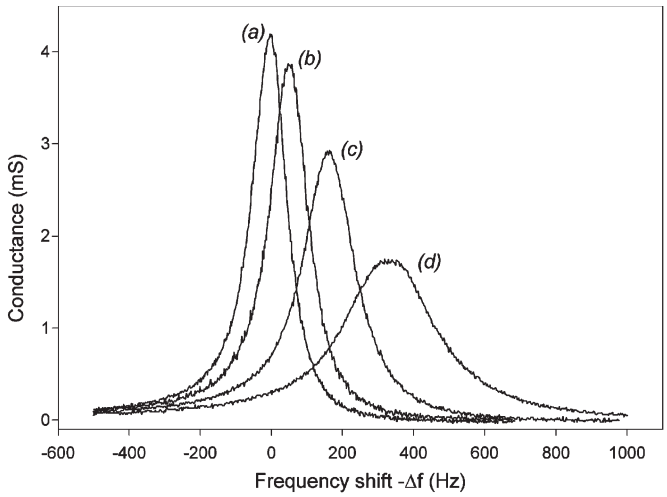

Fig. 4. Graph of conductance versus frequency shift for a QCM coated with PE-co-VA deposited from 5% v/v polymer solution (a) and exposed to methanol headspace vapors with concentrations of (b) 80, (c) 160, and (d) 320 ppm.

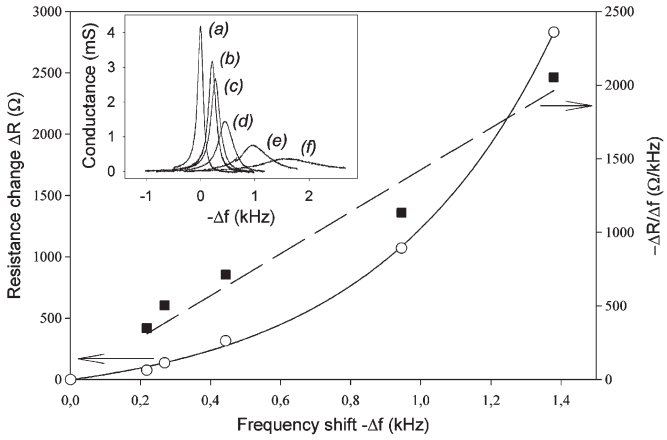

Fig. 5. Graph of resistance change ΔR ($\circ$) and $-\Delta R/\Delta f$ ($\blacksquare$) versus frequency shift $-\Delta f$ for a QCM sensor coated with PE-co-VA exposed to the first five primary alcohols. The inset graph is a plot of conductance versus frequency shift for the PE-co-VA sensor (a) and exposed to (b) methanol, (c) ethanol, (d) propanol, (e) butanol, and (f) pentanol.

shift increases, and the conductance peak broadens and reduces in size.

The effect of exposing a PE-co-VA-coated QCM sensor to methanol vapor is demonstrated by increasing the concentration from 80 to 320 ppm (Fig. 4). After allowing time for the odor entering and leaving the sensor polymeric matrix to equilibrate, the absorption of methanol into the sensor mirrors the deposition of the polymer onto the QCM. As the partial pressure of the methanol is increased, a larger quantity of the vapor is absorbed in the polymeric matrix causing the resonant frequency peak to move to lower frequencies. The conductance peak becomes broader and smaller as a consequence.

A QCM sensor coated with PE-co-VA deposited from 5% v/v polymer solution is used to illustrate the characteristic of the change in resistance ΔR ($\circ$) and the frequency shift $-\Delta f$ (Fig. 5). The ratio $-\Delta R/\Delta f$ is fitted using the exponential curve $y = 198.66 \exp^{1.98x}$. Furthermore, exposing the sensor to the headspace of the first five primary alcohols demonstrates

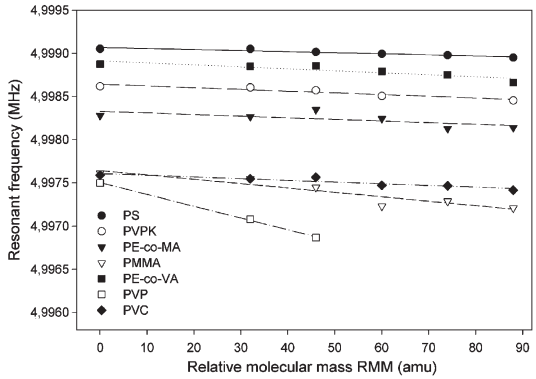

Fig. 6. Graph of resonant frequency versus relative molecular mass RMM for an array of QCM sensors.

the broadening and frequency shift of the conductance peaks due to an increase in mass for each gas (Fig. 5, inset graph).

The effect of exposing the same alcohol vapors to different polymer coatings is illustrated using an array of seven QCM sensors (Fig. 6). Each sensor is coated with a polymer, which is deposited from a 1% v/v solution of the polymer dissolved in the appropriate solvent. The QCM sensor array is then exposed to the headspace of the first five primary alcohol vapors at a concentration of 80 ppm. For each polymer-coated QCM sensor, the resonant frequency decreases linearly as the mass of the deposited odor increases.

IV. Discussion

The Butterworth van Dyke (BVD) electrical model [13] of a QCM resonator is used to analyze the admittance plots in Fig. 2. The model is made up of two branches, namely 1) the motional branch, which consists of a resistor r, an inductor l, and a capacitor c, all connected in series and 2) a shunt capacitor c_0. The motional branch, as the name suggests, describes the electromechanical properties of the QCM. Each of these parameters is an electrical equivalence of the physical properties of the crystal, which, together, can be used to determine the resonating characteristics of a crystal under certain experimental conditions. In the other branch, the shunt capacitor c_0 measures the static capacitances present in the overall system.

The overall admittance of the model is calculated using the method described by Taylor *et al.* [14], [15]. The real (conductance G) and imaginary (susceptance B) part of the admittance can be written with the components described in the BVD model as

$$G = \frac{\omega^2 r c^2}{(\omega^4 c^2 l^2) + (\omega^2 r^2 c^2) - (2\omega^2 cl) + 1} \tag{2}$$

$$B = \frac{(\omega^5 c^2 l^2 c_0) - (\omega^3 c^2 l) + (\omega^3 r^2 c^2 c_0)}{(\omega^4 c^2 l^2) + (\omega^2 r^2 c^2) - (2\omega^2 cl) + 1} - \frac{(2\omega^3 clc_0) - \omega c - \omega c_0}{(\omega^4 c^2 l^2) + (\omega^2 r^2 c^2) - (2\omega^2 cl) + 1}. \tag{3}$$

There are three important frequencies of interest in this application. The first is the resonant frequency of the BVD model, which is found at the point where the amplitude of G is at its maximum. The other two frequencies, which determine the bandwidth, are located at the points where the magnitudes of B are at a maximum. Alternatively, these two frequencies can also be found at the peak-width-half-height of the G spectrum. The fluctuations in these frequencies are a useful indication of the actual electromechanical changes that take place on the surface of the QCM.

TABLE II
Calculated Equivalent Circuit Component Values

Parameter	Impedance analyser	
	HP 4192A	*Custom-built*
r (Ω)	42.427064340	48.059397340
c (F)	$6.788255425\text{x}10^{-15}$	$4.583433833\text{x}10^{-15}$
c_0 (F)	$1.109557210\text{x}10^{-9}$	$1.259130010\text{x}10^{-10}$
l (H)	0.192497843	0.221113073

The component values of the BVD model for the admittances in Fig. 2 are extrapolated using the software Microcal Origin, which is supplied by Microcal Software Inc. This program uses a computational nonlinear curve fitting method that solves (2) and (3) to extrapolate the component values (Table II). The goodness-of-fit is monitored using the correlation coefficient to produce a final curve fitting of 99% confidence limit. Verification performed by replotting the admittance data using the extrapolated component values shows good correlation in the original admittance data measured with the custom-built analyzer [Fig. 2(a)] and the HP analyzer [Fig. 2(b)].

The values calculated for the custom-built analyzer are relatively close to those obtained from the calibrated HP analyzer, with the exception of the value for c_0. In the admittance plots, this difference is displayed by the relative inductive nature of the calculated susceptance for the custom-built analyzer. The reason is that admittances measured with this device are calculated using only the component values built into the circuitry. Hence, parasitic parameters due to interconnects and from the multiplexers of the QCM array are ignored in the calculation of c_0. Overall, however, the custom-built analyzer provides a sufficiently efficient solution for characterizing a QCM. In this application, the most critical element is the detection of resultant changes in admittance spectrum at the resonance region such as the subtle changes in the form of resonance shifts and amplitude reduction. These changes are easily detectable using the custom-built device as shown in the results of the remaining experiments.

Fig. 3 illustrates the results recorded from QCMs that were deposited with polymer films of different concentrations. There is an approximate linear increase in the resonant frequency as the concentration of the polymer film is increased. Similar trends are also recorded in Figs. 4 and 5 (inset graph) where the polymer-coated QCM was exposed to different concentrations of head gas and different primary alcohols, respectively. Each increase in the concentration of polymer film, increase in concentration of head gas, or increase in relative molecular mass (RMM) is reciprocated with a negative shift in resonance peak G, a reduction in the maximum amplitude of G, and the broadening of the bandwidth.

Shifts in resonance are reflected by changes in l and c because they are closely related to the oscillatory properties of the

crystals. The component r, which describes the frictional losses of the QCM, fluctuates with the different peak amplitudes of G. The fluctuations of r are explored in detail by exposing the polymer-coated QCMs to different RMMs of primary alcohols (Fig. 5). The change in r is found to be approximately linear to the frequency shift for the lower RMM primary alcohols. However, this relationship becomes logarithmic in nature for heavier RMM alcohols. The point at which the relationship becomes invalid is known as the viscoelastic limit. Thus, r is a damping factor that reflects the frictional losses due to mass loading. Hence, the viscoelastic limit is the point when the surface of the QCM becomes overdamped and oscillation becomes increasingly unsustainable as a result.

The quality factor Q is another parameter that is also used to describe the resonant behavior of a QCM. It is defined as the ratio between the resonant frequency and the bandwidth. Alternatively, it can be calculated from the component values of the BVD model [16] using

$$Q = \frac{\omega_0 l}{r} = \frac{\omega_0}{\omega_2 - \omega_1} \tag{4}$$

where ω_0 is the point at which the resonant frequency is a maximum in the conductance plot, and ω_1 and ω_2 are the frequencies at half the height of the conductance peak at either side of the maximum. In general, an increase in the mass deposited on the surface of the QCM reduces the Q calculated for the QCM. This indicates a degrading effect to the quality of the QCM as a resonator. This trend is observed in the results that were obtained from the experiments that produced the data presented in Figs. 3–5.

The admittance spectrum in Fig. 3 is obtained from the QCMs coated with different concentrations of PE-co-VA films. The Q for an uncoated QCM is 1.6×10^5, whereas the Q for a coated QCM with 5% solution is 3.8×10^4. Similarly, by changing the type of exposure, whether it is through increasing the concentration of head gas (Fig. 4) or increasing the RMM of primary alcohols (Fig. 5), the values of Q reflect an inverse proportionality. In Fig. 4, Q decreases from 3.8×10^4 to 1.6×10^4 when it is exposed to 320 ppm methanol. In Fig. 5, Q decreases to 8320 for propanol and 3570 for pentanol, both less than the viscoelastic limit of 1×10^4. Hence, in general, the value of Q degrades as the load on the surface of the QCM increases.

Lucklum and Hauptmann have used the $\Delta f - \Delta R$ technique [17] to investigate the material property changes due to thickness or mass changes. They have demonstrated this method to show good distinction between a glassy film and a viscoelastic polymer film [18]. From Fig. 5, the results of detecting methanol, ethanol, and propanol suggest a linear change in $\Delta f - \Delta R$, but butanol and pentanol recorded a larger change in ΔR with respect to Δf. By comparison to the results in [18], increasing RMM changes from butanol onward has resulted in severe viscoelastic contribution, where the rate of ΔR changes faster than Δf. This implies that the use of the Sauerbrey equation is insufficient to predict the responses from any further increase of RMM. Despite this limitation, the data clearly show that the system has excellent discriminatory abilities for light alcohols.

TABLE III
SENSITIVITY AND PERMEATIVITY OF POLYMER-COATED QCM SENSORS

Polymer	Sensitivity / Hz amu^{-1}	Permeativity [19] / cm^3 (@STP) cm cm^{-2} s^{-1} Pa^{-1}
PS	−1.22	1350x10^{-13}
PE-*co*-MA	−1.89	
PVC	−1.97	206x10^{-13}
PVPK	−1.99	
PE-*co*-VA	−2.30	
PMMA	−5.05	480x10^{-13}
PVP	−13.57	

In order to extend the linear measuring range of the polymer-coated QCMs, 1% v/v solutions were used in place of the 5% v/v solutions to reduce the initial polymer film thickness. The responses of the QCM sensors when exposed to headspace alcohols with increasing RMM are shown in Fig. 6. All polymer types that were used in the experiment exhibited a linear shift in Δf with respect to alcohol vapors ranging between an RMM of 0 and 90. The sensitivity values as shown in Table III were calculated from the slopes of each of the responses in Fig. 6. The magnitude of the changes in the values are dependent on the hydrophilicity of the sensor polymer coating.

The polyvinylpyrrolidone (PVP) polymer film is the most hydrophilic of the polymers used here and, as such, shows the greatest change in QCM resonant frequency upon increasing the mass of the alcoholic vapor. The other polymers are less hydrophilic, and hence, display a smaller decrease in frequency as the vapor mass increases. In the case of PVP, H-bond formation is facilitated by stabilization of the N–C bond, in the $-\mathrm{N}-\mathrm{C}=\mathrm{O}$ moiety of the pyrrolidone, via electron donation from the nitrogen atom. This may occur in polymers such as polymethylmethacrylate (PMMA) and PE-co-VA to a lesser extent, but the presence of long hydrocarbon chains (e.g., in polyethylene-co-methylacrylic acid (PE-co-MA) and PE-co-VA) or a lack of an oxygen atom in the polymeric structure [e.g., in polystyrene (PS)] makes them increasingly hydrophobic. Indeed, the sensitivity of the PE-copolymers may depend on the amount of PE in the structure as PE-co-MA contains 71% PE and produces a less sensitive alcohol sensor than PE-co-VA with 66% PE.

Permeativity data for PS, polyvinylchloride (PVC), and PMMA, which are reproduced in Table III [19], give an idea of the density of these polymer films. The high permeativity of PS suggests that the alcohol vapors should penetrate the film and interact easily with the polymer. However, the low affinity of PS for alcohols means that the sensor sensitivity is low. PVC has a much lower permeativity, which means that interactions between the odorant and itself would mainly be limited to the sensor surface, but again, the inability to form H-bonds to the alcohol means that the sensor sensitivity is low. PMMA has a higher affinity for the vapors and therefore a higher sensitivity than the other two polymers, even though it has a lower permeativity than PS. The sensitivity of the sensor is therefore mainly dependent on the ability of the polymer to

form H-bonds with the alcohol odorant, rather than on steric constraints.

V. Conclusion

We have presented a prototype impedance analyzer that uses a multiplexing bridge circuit for extracting the impedance spectrum from an array of polymer-coated QCM sensors. The analyzer can characterize a QCM sensor by measuring the conductance and susceptance in the presence of headspace primary alcohol vapors. The impedance analyzer is a versatile instrument, which is constructed on a single PCB and is sufficiently small enough to be integrated into a handheld unit. The system has been tested using an array of QCMs that were functionalized to yield different characteristic responses. Consequently, by choosing different polymers, it is possible to distinguish between various compounds and changes in concentrations. Hence, we envisage that the analyzer could be combined with a QCM sensor array to realize a cheap handheld electronic nose device for the detection of different gases.

Acknowledgment

The authors would like to thank Dr. C. Wyse (University of Glasgow, U.K.), for practical guidance on fabricating the polymer-coated QCM sensors, and Prof. D. M. Taylor (University of Wales, U.K.), for the technical advice on impedance measurements.

References

[1] K. J. Albert, N. S. Lewis, C. L. Schauer, G. A. Sotzing, S. E. Stitzel, T. P. Vaid, and D. R. Walt, "Cross-reactive chemical sensor arrays," *Chem. Rev.*, vol. 100, no. 7, pp. 2595–2626, Jul. 2000.

[2] J. W. Grate and M. H. Abraham, "Solubility interactions and the design of chemically selective sorbent coatings for chemical sensors and arrays," *Sens. Actuators B, Chem.*, vol. 3, no. 2, pp. 85–111, Feb. 1991.

[3] M. Cole, G. Sehra, and J. W. Gardner, "Development of smart tongue devices for measurement on liquid properties," *IEEE Sens. J.*, vol. 4, no. 5, pp. 543–550, Oct. 2004.

[4] J. S. Danel and G. Delapierre, "Quartz: A material for microdevices," *J. Micromech. Microeng.*, vol. 1, no. 4, pp. 187–198, Dec. 1991.

[5] L. Cui, M. J. Swann, A. Glidle, J. R. Barker, and J. M. Cooper, "Odour mapping using microresistor and piezo-electric sensor pairs," *Sens. Actuators B, Chem.*, vol. 66, no. 1–3, pp. 94–97, Jul. 2000.

[6] M. J. Swann, A. Glidle, L. Cui, J. R. Barker, and J. M. Cooper, "The determination of gaseous molecular density using a hybrid vapour sensor," *Chem. Commun.*, no. 24, pp. 2753–2754, Dec. 1998.

[7] P. Horowitz and W. Hill, *The Art of Electronics*, 2nd ed. Cambridge, U.K.: Cambridge Univ. Press, Jul. 1989.

[8] H. Bresch, F. Eichelbaum, J. Schröder, W. Mathis, and P. Hauptinann, "A new concept of sensor interface electronics for resonant sensors," in *Proc. Eurosens. XIII*, Sep. 1999, pp. 265–266.

[9] A. Sabot and S. Krause, "Simultaneous quartz crystal microbalance impedance and electrochemical impedance measurements. Investigation into the degradation of thin polymer films," *Anal. Chem.*, vol. 74, no. 14, pp. 3304–3311, Jul. 2002.

[10] A. Arnau, T. Sogorb, and Y. Jiménez, "A new method for continuous monitoring of series resonance frequency and simple determination of motional impedance parameters for loaded quartz-crystal resonators," *IEEE Trans. Ultrason. Ferroelectr. Freq. Control*, vol. 48, no. 2, pp. 617–623, Mar. 2001.

[11] J. Schröder, R. Borngräber, F. Eichelbaum, and P. Hauptmann, "Advanced interface electronics and methods for QCM," *Sens. Actuators A, Phys.*, vol. 97–98, pp. 543–547, Apr. 2002.

[12] M. P. Martí, R. Boqué, O. Busto, and J. Guasch, "Electronic noses in the quality control of alcoholic beverages," *Trends Anal. Chem.*, vol. 24, no. 1, pp. 57–66, Feb. 2005.

[13] J. Henderson, *Electronic Devices. Concepts and Applications*. Englewood Cliffs, NJ: Prentice-Hall, 1991, p. 357.

[14] D. M. Taylor and H. L. Gomes, "Electrical characterization of the rectifying contact between aluminium and electro-deposited poly(3-methylthiophene)," *J. Phys. D, Appl. Phys.*, vol. 28, no. 12, pp. 2554–2568, Dec. 1995.

[15] D. M. Taylor and C. A. Mills, "Memory effect in the current-voltage characteristic of a low-band gap conjugated polymer," *J. Appl. Phys.*, vol. 90, no. 1, pp. 306–309, Jul. 2001.

[16] D. A. Buttry and M. D. Ward, "Measurement of interfacial processes at electrode surfaces with the electrochemical quartz crystal microbalance," *Chem. Rev.*, vol. 92, no. 6, pp. 1355–1379, Sep./Oct. 1992.

[17] R. Lucklum and P. Hauptmann, "The $\Delta f - \Delta R$ technique: An approach to an advanced sensor signal interpretation," *Electrochim. Acta*, vol. 45, no. 22–23, pp. 3907–3916, Jul. 2000.

[18] R. Lucklum, C. Behling, and P. Hauptmann, "Role of mass accumulation and viscoelastic film properties for the response of acoustic-wave-based chemical sensors," *Anal. Chem.*, vol. 71, no. 13, pp. 2488–2496, Jul. 1999.

[19] *Polymer Handbook*, 4th ed. J. Brandrup, E. H. Immergut, E. A. Grulke, and D. R. Bloch, Eds. New York: Wiley, Feb. 1999, p. VI/437. Table C.

Christopher A. Mills received the B.Sc. degree in chemical science from the University of Salford, Salford, U.K., in 1996 and the Ph.D. degree in the electronic properties of semiconducting polymers from the University of Wales, U.K., in 2000.

He was with the University of Glasgow, Glasgow, U.K., as a Postdoctoral Researcher, studying polymer-based electronic nose technology. He is currently with the Barcelona Science Park, Barcelona, Spain, as a Postdoctoral Researcher, working in the field of polymer-based nanotechnology.

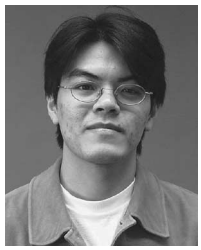

Kevin T. C. Chai received the B.Eng. (Hons.) degree in electronic and electrical engineering from the University of Glasgow, Glasgow, U.K., in 2002. He is currently working toward the Ph.D. degree in the Microsystem Technology Research Group, University of Glasgow, where he is developing integrated biosensor array chips for tomographic bioimpedance imaging of cell cultures.

His research interests include bioimpedance imaging methods, silicon-based system design, and biomedical engineering.

Mark J. Milgrew (M'04) received the M.Eng. (Hons.) degree in electronic and software engineering from the University of Glasgow, Glasgow, U.K., in 2001.

He was a Product Design Engineer with General Electric in the U.K. and in the USA, where he gained international experience in the industry. He is currently with the Glasgow Electronics Design Centre, University of Glasgow, as a Research Fellow. His research interests include electronics design, integrated sensor systems, cell-based biosensors, and biomedical engineering.

Mr. Milgrew is a member of the IEE.

Andrew Glidle received the B.Sc. and Ph.D. degrees from the University of Exeter, Exeter, U.K., in 1984 and 1988, respectively, and is a CChem and MRSC.

He has developed a number of analytical methods in the fields of electrochemistry, physical chemistry, materials science, and bioelectronics, together with various methods for the specific immobilization of chemical or biological motifs on sensors surfaces. He is currently a Research Technologist in the Bioelectronics Research Group, University of Glasgow, Glasgow, U.K.

Jonathan M. Cooper received the B.Sc. degree in biological sciences from the University of Southampton, Southampton, U.K., in 1983 and the Ph.D. degree in sensor technology from the University of Cranfield, Cranfield, U.K., in 1989.

He is currently a Professor of bioelectronics with the Department of Electronics and Electrical Engineering, University of Glasgow, Glasgow, U.K. His current research interests include lab-on-a-chip technologies and bionanotechnology.

Prof. Cooper is a Fellow of the Royal Society of Edinburgh and of the Royal Academy of Engineering.

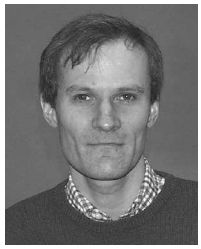

David R. S. Cumming (M'97) received the B.Eng. degree from the University of Glasgow, Glasgow, U.K., in 1989 and the Ph.D. degree from the University of Cambridge, Cambridge, U.K., in 1993.

He has worked variously on mesoscopic device physics, radio frequency characterization of novel devices, fabrication of diffractive optics for optical and submillimeter-wave applications, diagnostic systems, and microelectronic design. He is currently a Professor and an EPSRC Advanced Research Fellow in Electronics and Electrical Engineering at the University of Glasgow, where he leads the Microsystem Technology Research Group.